AD-A144 857   NONLINEAR ULTRASONIC CHARACTERIZATION OF OXYGEN   1/1
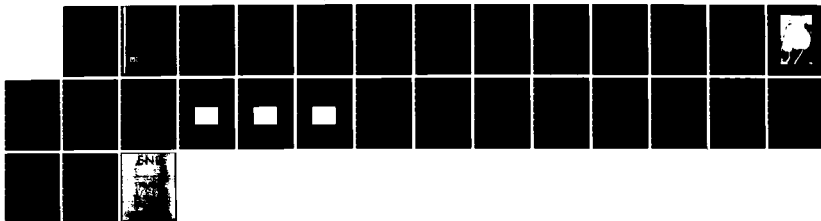IMPURITIES IN TITANIUM II..(U) UNITED TECHNOLOGIES
RESEARCH CENTER EAST HARTFORD CT
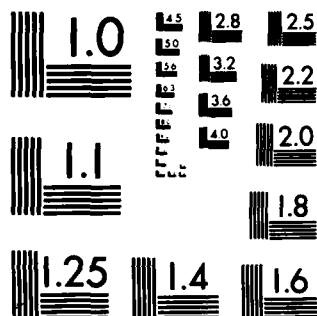UNCLASSIFIED   H I RINGERMACHER ET AL. SEP 83   F/G 11/6   NL

MICROCOPY RESOLUTION TEST CHART

NATIONAL BUREAU OF STANDARDS-1963-A

$E\text{ool}\text{c}45$

(4)

NONLINEAR ULTRASONIC CHARACTERIZATION OF OXYGEN IMPURITIES IN TITANIUM, II

FINAL REPORT
R83-996217
SEPTEMBER 1983

Naval Research Laboratory

Contract N00014-82-C-2346

UNITED TECHNOLOGIES RESEARCH CENTER

East Hartford, Connecticut 06108

83 10 24 023

R83-996217

Nonlinear Ultrasonic Characterization of
Oxygen Impurities in Titanium, II

Final Technical Report

Prepared for

Naval Research Laboratory

Contract N00014-82-C-2346

REPORTED BY _Harry I. Ringermacher_
Harry I. Ringermacher
Associate Research Engineer

APPROVED BY _Robert K. Erf_
Robert K. Erf
Supervisor, Optics and
Acoustics

DATE September 1983

NO. OF PAGES _ _ _   COPY NO. _____

R83-996217

FORWARD

letter on file

A-1

i

R83-996217

Nonlinear Ultrasonic Chracterization of Oxygen Impurities in Titanium, II

TABLE OF CONTENTS

R83-996217

Nonlinear Ultrasonic Characterization of
Oxygen Impurities in Titanium, II

SUMMARY

   Titanium specimens containing oxygen impurities ranging from 0.1 to 0.3
percent by weight have been examined using nonlinear ultrasonic techniques.
The amplitude of the second harmonic ultrasonic response has been observed
to deviate from the expected perfect square law behavior. The increasing
deviation correlates well with increasing oxygen contamination.
Measurements of third harmonic generation showed no significant correlation
with oxygen content. Following a brief review of the important results and
an introductory section, the theory, experimental techniques and test
results are presented in detail.

RESULTS AND CONCLUSIONS

Nonlinear second harmonic ultrasonic techniques were applied to determine the presence of oxygen impurities in five titanium specimens provided by the Naval Research Laboratory. The major results of the program are summarized below.

1. For a fixed average grain size, the ultrasonic second harmonic amplitude in oxygen contaminated titanium was found to deviate from expected perfect square law dependence. The deviation increased with increasing oxygen content. This confirms the square law deviation observed in the study reported in Ref. 1. Since a different type of apparatus was used in the present work, the conviction that the observation is specimen related is strengthened.

2. Evidence of grain size effects was detected in the experiments. Average grain size in the present study ranged from 700 μm in specimen A to 300 μm in specimen E, while varying between 100 μm and 10 μm in the first study. The overall level of square law deviation was approximately twice as great in the present study than in the study reported in Ref. 1. This suggests a dependence of the overall level of square law deviation on grain size.

3. Measurements of the third harmonic amplitude as a function of oxygen concentration showed relatively little change, thus indicating third harmonic generation is not responsible for the apparent square law deviation of the second harmonics. These results leave open the question of the physical cause of the square law deviation. One possibility is the presence of grain-size-induced local residual stresses in the titanium. This is discussed more extensively in the theory section of the report.

INTRODUCTION

The presence of oxygen in titanium alloys is known to alter their material properties. Oxygen concentrations as low as 0.1 wt% dramatically increase the strength and hardness of these alloys (Ref. 2). At the same time, however, the alloy ductility is decreased (Ref. 3). These effects are particularly important at weld sites where oxygen embrittlement can pose a serious problem when contamination occurs. The level of contamination will determine the severity of embrittlement. It is, therefore, desirable to seek a simple, nondestructive, field-worthy technique with high sensitivity to the presence of oxygen impurities in these alloys.

Ultrasonic techniques generally satisfy this latter demand. Hardness and internal friction must influence both the sound velocity and the attenuation - frequency spectra in these materials. At the very least, the presence of oxygen is expected to change the density and, hence, the sound velocity. In addition, oxygen should alter the elastic constants, although observation of this effect can be more complicated.

Velocity of sound methods have been shown capable of measuring oxygen content in titanium (Ref. 4). The responsible mechanisms in this case were approximately equal proportions of density and elastic constant changes with increasing oxygen content. The results were most accurate for the measurement of oxygen content from 0.3 wt% to 1.0 wt%. Below 0.3 wt%, where all of the present research is concentrated, the velocity of sound approach encountered large errors and showed no significant correlation to oxygen content.

Nonlinear ultrasonic methods have an advantage over linear methods, such as velocity and attenuation measurement, in that the power law dependence of the second harmonic amplitude, for example, is independent of such factors as specimen surface preparation, transducer bond quality and, to a large extent, grain structure (Ref. 5). Since it has been shown that the ultrasonic harmonic amplitude can be influenced by specimen impurities (Refs. 6 and 7), these advantages might serve to improve sensitivity to low level oxygen concentrations.

3

THEORY

The nonlinear approach of the earlier work (Ref. 1), was based on the assumption that oxygen acts upon the dislocations either by pinning or by generating localized stresses and thereby altering the third harmonic content of the observed ultrasonic signal. If perfect square law behavior for second harmonic generation is assumed, then the presence of third harmonics, dependent on oxygen content, will appear as a deviation from square law behavior and vary monotonically as a function of the oxygen concentration in the titanium specimens. These effects were predicted and measured by Hikata. It is well known that motions of dislocations in single crystals can be a source of second harmonic generation (Ref. 6). Hikata has shown (Ref. 7) that the presence of impurities can pin dislocation motion thereby altering both the second and third harmonic content. Grain size in a polycrystalline sample may also have an effect on harmonic generation. Jon, et al., (Ref. 5), have shown that 99.96 percent pure polycrystalline titanium demonstrates a strict square law second harmonic behavior, apparently arising from lattice anharmonicity.

Thus, the deviation from square law behavior observed in the earlier work, and its strong correlation to oxygen content, suggested a follow up search for possible direct effects upon the third harmonics. Hikata showed (Ref. 8) that as dislocation loop lengths shortened from a known upper limit, the third harmonic content increased. Since oxygen can act as an impurity to pin a dislocation loop and thereby shorten it, an increasing oxygen content was expected to cause an increase in the third harmonics. However, no significant change in third harmonic level was observed in the present work. Therefore, this hypothesis was excluded.

In the work of Ref. 1, an alternative possibility was mentioned: i.e. stresses induced by the oxygen in the nature of local residual stress. This might also cause the observed results directly, through effects on the second harmonics. The second harmonic amplitude, A_2, can be written in the following form (Ref. 7):

$$A_2 = K_2 (X^2 + Y^2 - 2BXY) A_{10}^2 \, f_2(\alpha, x), \qquad (1)$$

where K_2 is a constant for fixed operating conditions; A_{10} is the acoustic amplitude of the fundamental at $x = 0$, the starting point of the wave; and $f_2(\alpha, x)$ is an attenuation factor depending upon the attenuations, α, (x) and $\alpha_2(x)$, of the fundamental and second harmonics as a function of position.

4

X^2 is the lattice anharmonicity term and is always present in both single crystals and polycrystalline materials. Y^2 is the dislocation loop term. This term is expanded below to show the important contributing factors.

$$Y^2 = C \left[\frac{NA_o}{L_o^2} \right]^2 , \tag{2}$$

where C is a constant dependent upon fixed operational parameters and material properties; N is the dislocation loop density; L_o is the dislocation loop length; and A_o is the applied bias stress. The last term in Eq. (1), XY, is an interaction term. In near perfect single crystal lattices, where dislocation loop density is very low, the anharmonic term dominates. In polycrystalline materials, the dislocation contribution can be large and both will contribute. However, the anharmonic term will remain relatively constant as parameters such as impurity content vary for low concentrations. It is important to note that a bias stress A_o must be applied in order for the Y^2 term to contribute to the second harmonic generation. The stresses in the material in the presence of an acoustic wave can in general be written as

$$c = A_o + A_1 \cos(\omega t - kx) + A_2 \cos(\omega t - kx - \delta_2) + A_3 \cos(\omega t - kx - \delta_3) , \tag{3}$$

where A_1, A_2 and A_3 are the peak acoustic amplitudes of the fundamental, second and third harmonics respectively; is the ultrasonic frequency; $k = 2\pi/\lambda$ is the wavenumber; λ is the wavelength and δ is a phase angle. Although A_o is usually taken to be an _externally_ applied stress, there is no a-priori reason that it cannot be taken as a _local_ residual stress – local in the sense of the region in the vicinity of a grain seen by the acoustic wave of fundamental amplitude A_1 and wavelength λ. It is essential, however, that these stresses do not randomly average to zero over a region of length λ. In the present work, this is indeed the case where λ is approximately 0.5 mm, as is the grain size.

The third harmonic amplitude can be written in a form similar to the second harmonious amplitude:

5

$$A_3 = K_3 NA_{10}^3 \, f(L_o) f_3(\alpha, x), \tag{4}$$

where K_3 is, once again, constant for the operating conditions; $f(L_o)$ is dependent only on the dislocation loop length and f_3 is the attenuation factor correction for the third harmonic propagation given by,

$$f_3 = \left[\frac{e^{-3\alpha_1 x} - e^{-\alpha_3 x}}{\alpha_3 - 3\alpha_1} \right], \tag{5}$$

where α_3 is the third harmonic attenuation. The original hypothesis relied on the factor $f(L_o)$ for possible effects of the oxygen variations. $f_3(\alpha, x)$ is necessary for the third harmonic data analysis to properly take into account fundamental and third harmonic signal lost through specimen attenuation. This correction is extremely important in the present work, since the third harmonic datas are highly sensitive to attenuation effects on the fundamental.

EXPERIMENTAL TECHNIQUES

Specimens and Transducers

Five titanium specimens with wt.% oxygen contents of 0.075 (specimen A), 0.136 (B), 0.194 (C), 0.238 (D), and 0.290 (E), supplied by NRL, were machine ground, and lapped flat and parallel in preparation for the ultrasonic tests. In addition, the specimens were slowly annealed so that all would receive similar thermal histories resulting in more uniform grain size. The acoustic path length was 1.849 cm. The specimens were 6 in. long and of square cross section. The specimen oxygen content and measured sound velocity, are summarized in Table I.

Lithium niobate ($LiNbO_3$) transducers were used for all the nonlinear data collection. A 1.25 cm dia, 5 MHz. 36° -Y cut transducer was used as the transmitter for longitudinal waves. The receiver for the second harmonic data, bonded on the opposite side of the plate, was a similar 0.625 cm dia, 10 MHz transducer. All the transducers were bonded with Nonaq grease and "wrung in." The transducer bond to the optical quality fused quartz delay block used in taking the third harmonic data was made with "Salol", thus ensuring a thin, rigid bond. The 2.54 cm dia. x 1.27 cm long delay block was then Nonaq-bonded to the specimens. The specimen and block were placed on a polystyrene support base (Fig. 1) and a second support of identical construction was placed on the top of the specimen making contact around the transducer. In this way, pressure was applied to the assembly to permit control of the Nonaq bond thickness. Contact to the transducers was made through fine wires spot-soldered on the ground side and center of the coaxial plating.

FIG. 1

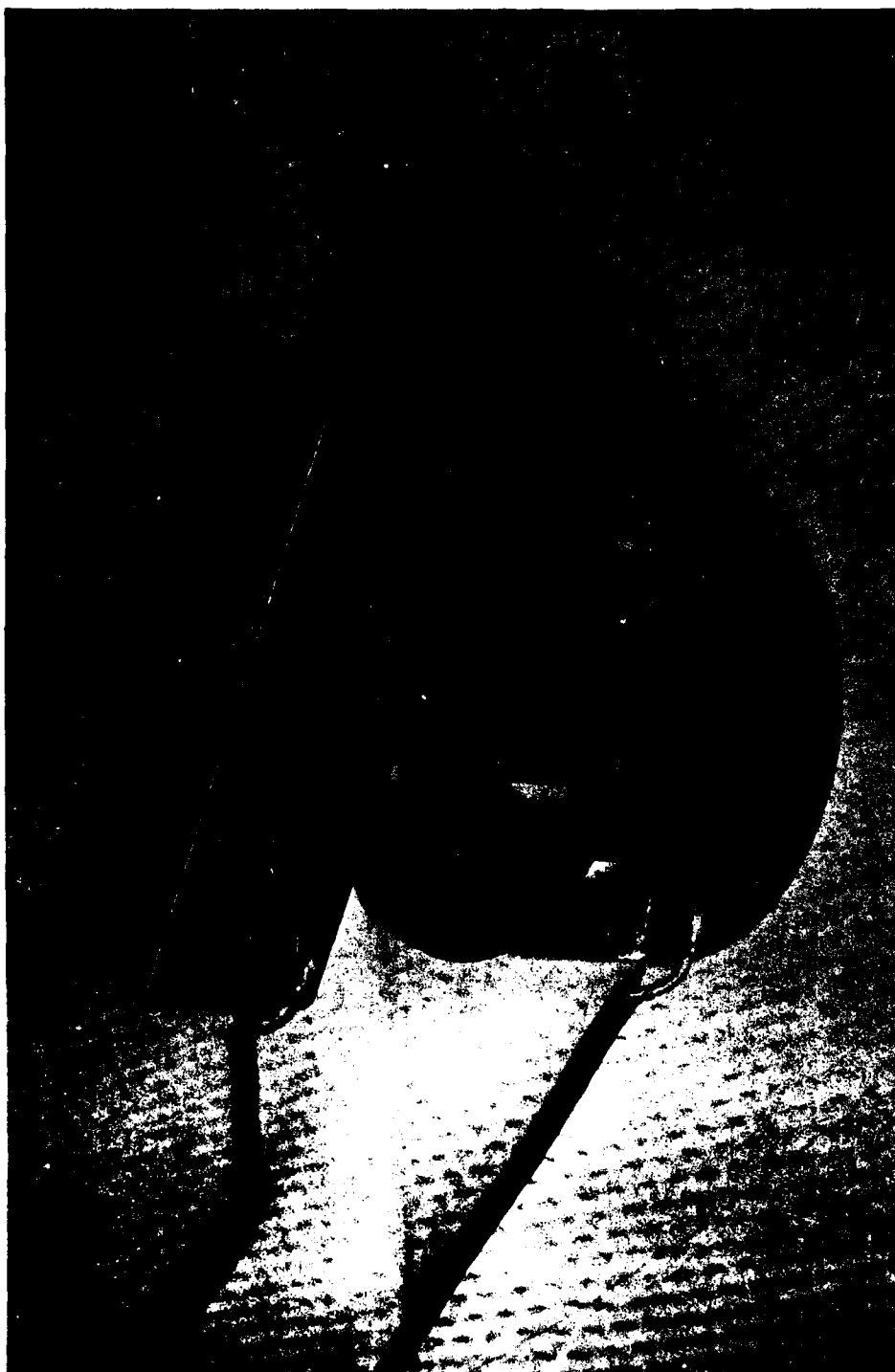TI SPECIMEN/QUARTZ DELAY ASSEMBLY USED FOR THIRD HARMONIC DATA

83—8—13—12

8

TABLE I

SUMMARY OF SPECIMEN PROPERTIES

| Specimen	Oxygen Content, Wt%	Longitudinal Sound Velocity, cm/sec
A	0.075	$(5.95 \pm 0.05) \times 10^5$
B	0.136	5.95 ± 0.05
C	0.194	5.95 ± 0.05
D	0.238	$5.95 + 0.05$
E	0.290	5.95 ± 0.05

Instrumentation

A block diagram of the ultrasonic system assembled for the nonlinear measurements is shown in Fig. 2. In the earlier work, a gated RF amplifier was used to generate the high power pulses. In the present work, a linear high power RF amplifier (ENI, MODEL A-300) was used in conjunction with separate mixer-controlled gating circuits to provide a 400 volt peak-to-peak gated RF pulse. The 2 μs long, 5 MHz RF pulse is shown in Fig. 3 after 5 MHz low-pass filtering. No observable second harmonics down to 45 dB below the fundamental entered the transducer (Fig. 4). Quartz and lithium niobate are known to respond very linearly at high powers so that it can be assumed that the bulk of second harmonics seen at the receiver transducer arises from the titanium specimen itself. Alan 50HT82.5 high power attenuators on the input and output sides permitted precisely controlled attenuation changes for calibration control of the data. New attenuators were used and calibration within the apparatus was carefully checked to ensure correct matching and switching linearity. In this way, the attenuator switch combinations could be made to reproduce performance within 0.25 dB. The input pulse was sent through a 5 MHz lowpass filter to inhibit transmission of 10 MHz rf, and the received signal for the second harmonic data was passed through a 10 MHz high pass filter to eliminate the 5 MHz fundamental transmission signal while permitting passage of any second harmonic 10 MHz rf generated within the sample as a result of its nonlinear response. (A 15 MHz bandpass filter was used in place of the 10 MHz high pass filter for the third harmonic studies.) A Matec 251 tuned preamp further restricted the bandwidth. A Matec 605 broadband receiver was used for the final gain stage to a recording instrument.

A typical pulse-echo response at 5 MHz in specimen E is shown in Fig. 5. An exponential decay function, produced by a decay generator, is shown on the same scope trace and was used to determine the attenuation of the fundamental and third harmonics necessary for corrections of the third harmonic data.

Procedures

It was important, in taking the nonlinear data, to ensure that the observed nonlinear behavior was not generated in the electronic equipment. To avoid this, the receiver amplifier was always operated at or near a fixed point on its response curve, for all input signal levels. It was assumed in taking the second harmonic data, that the second harmonic amplitude A_2 is precisely proportional to the square of the fundamental, A_1:
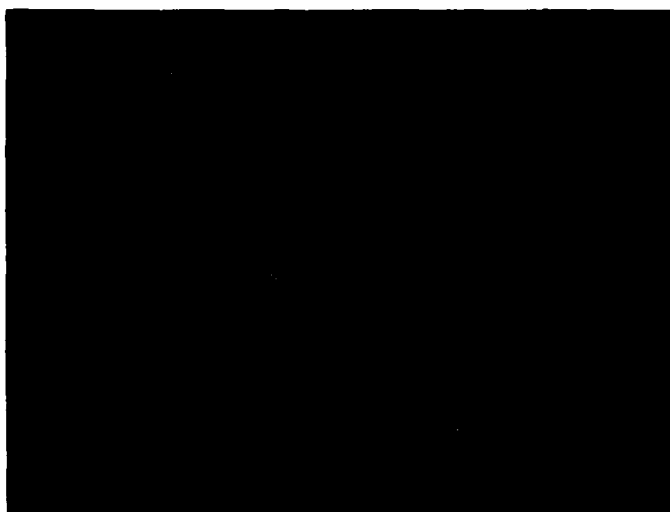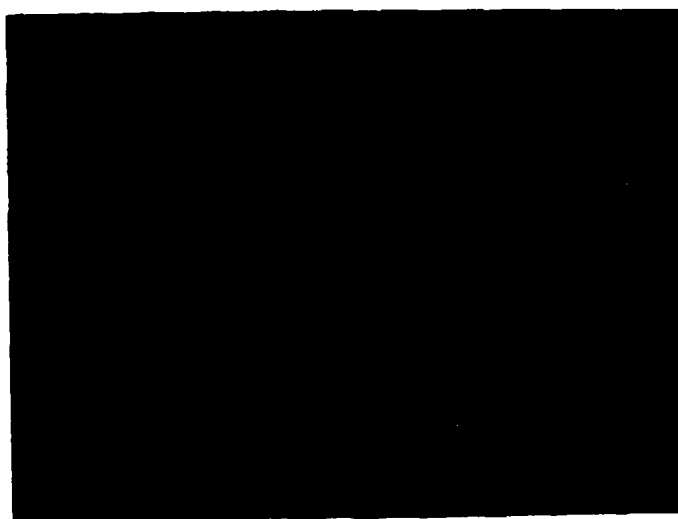
FIG. 2

ULTRASONIC SYSTEM FOR ANALYSIS OF MATERIAL NONLINEARITY

83—8—13—4

11

FIG. 3
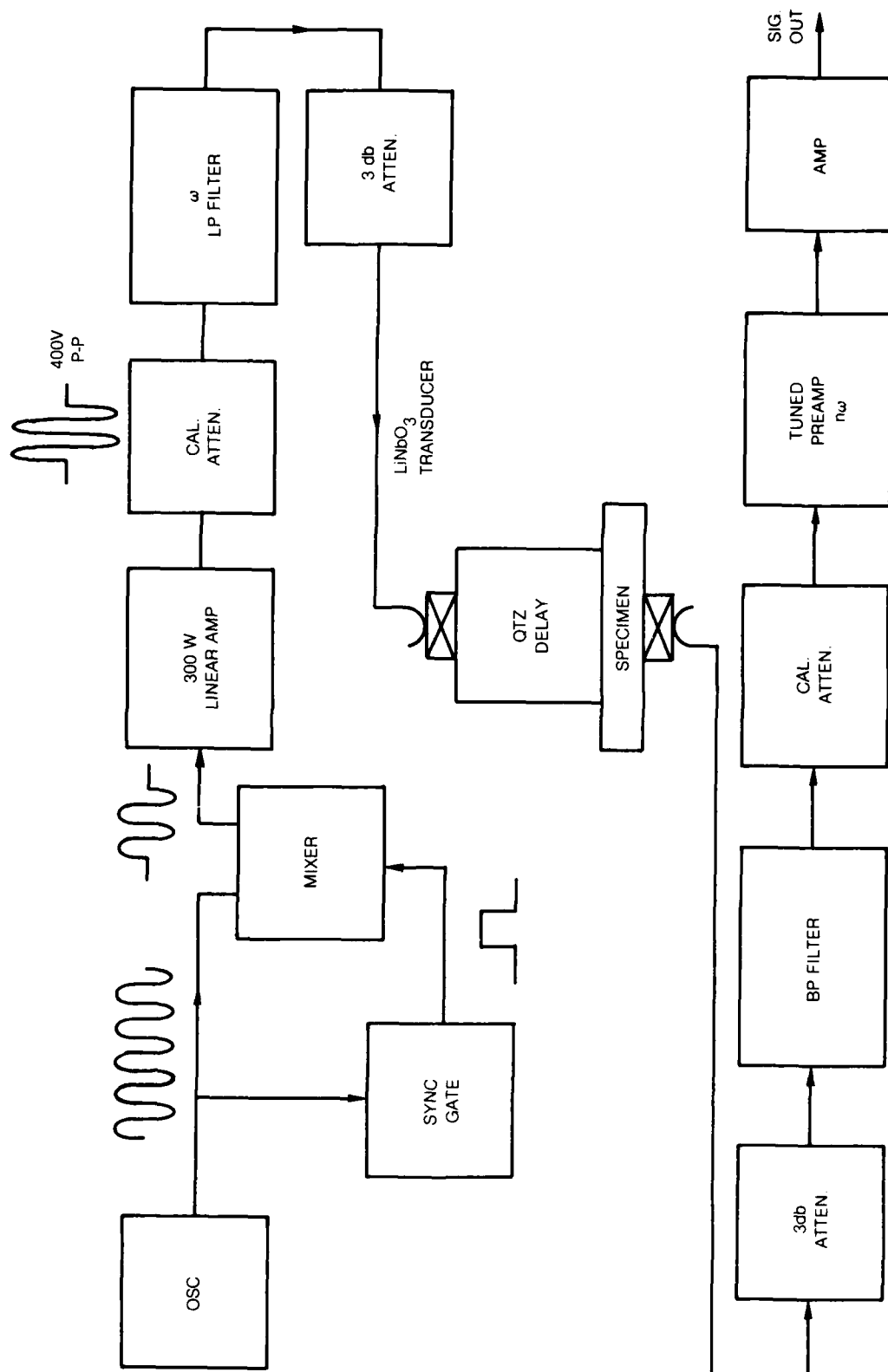
TRANSDUCER INPUT PULSE FROM LP FILTER

(400 VOLTS P-P, 5 MHz, 0.5μS/DIV)

83-8-13-2

FIG. 4

SPECTRAL CONTENT OF TRANSDUCER INPUT PULSE
AMPLITUDE (10 dB/DIV) VS FREQUENCY (2 MHz/DIV)

83—8—13—3

FIG. 5

PULSE-ECHO RESPONSE IN Ti SPECIMEN E

(5 MHz. 5µS/DIV)

83—8—13—1

$$A_2 = KA_1^{2.000} \tag{6}$$

Starting at the highest power level to the input transducer, 2.0 dB was withdrawn on the output side for every 1.0 dB of attenuation inserted at the input side. This fixed the exponent of Eq. (6) at 2.000. In this manner, a perfect square law response would correspond to a constant output signal level independent of the input signal level. Matching the attenuators as just described, and using lithium niobate, which is known to have an extremely linear response at high power levels, further helped to ensure valid results. System linearity was monitored at each new power level, and maintained to within two percent.

As seen in Eq. (4), the third harmonic amplitude is proportional to the cube of the fundamental. Thus, a small change in the fundamental is amplified threefold in the third harmonic. It is important to note that these refer to acoustic changes, and not merely electrical input to the transducer. The Nonaq bond was the source of greatest uncertainty in this regard. For a fixed voltage into the transducer, large variations in acoustic amplitude could be generated depending upon bond thickness. To control this, the quartz/specimen interface echo was continuously monitored on the input side. Pressure on the block was varied for each specimen to adjust the bond thickness so as to maintain a fixed echo amplitude for a constant voltage to the transducer. In this way, the input acoustic amplitude was maintained constant within 5% resulting in an intrinsic 15% variation in the third harmonic amplitude. Thus, any changes smaller than 15% deriving from oxygen effects, would not be detectable.

To improve test reliability, three points on each specimen were averaged for the attenuation data and the specimens were randomly chosen for analysis. In the Ref. 1 study, only one point on each specimen was used for the attenuation data.

15

EXPERIMENTAL RESULTS

Data were obtained over an input amplitude range of 12 dB with a maximum input voltage to the transducer of approximately 400 volts peak-to-peak. The input amplitude was decreased from its maximum value in 2.0 dB steps, while output attenuation was simultaneously decreased in 4.0 dB steps. To first-order, the output amplitude remained constant, thus indicating an approximate square law output behavior with input change. Since the deviation was small, a statistical method that disregards the quantitative nature of the deviation within each sample data set was employed. An average output amplitude A_2 was calculated for each sample using the power levels evaluated. The deviation of each amplitude level from the average output amplitude was taken to be a statistical representation of the deviation from perfect square law behavior, and a mean square deviation, ΔA_2, was calculated for each sample. The mean square deviation was then translated into an exponent deviation, ΔN, given by:
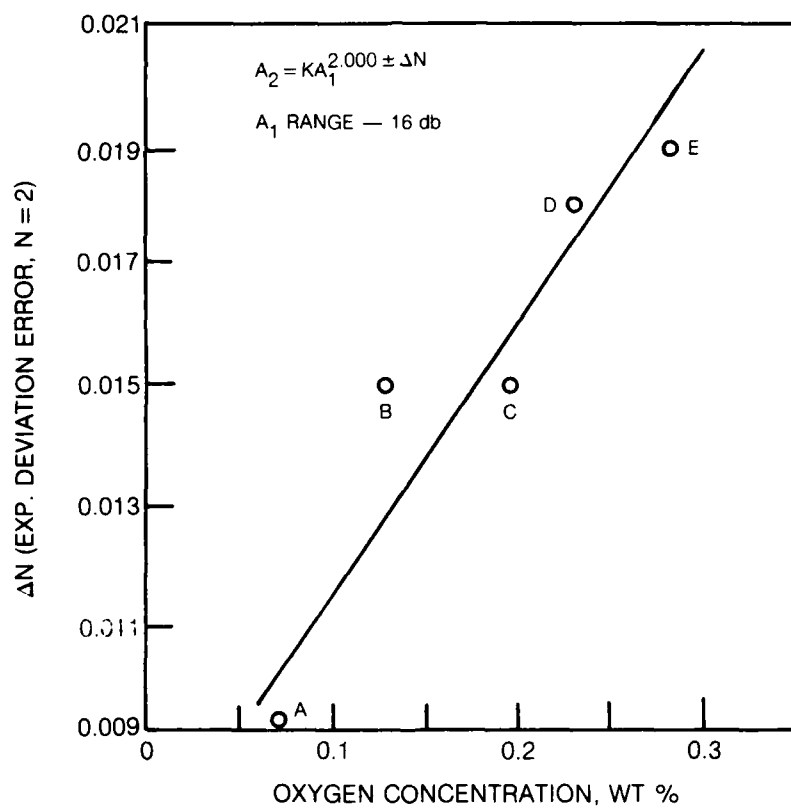
$$\Delta N = \left[\frac{\Delta A_2}{A_2}\right]\left[\frac{Ln\,10}{20}\right]\left[\frac{1}{<\alpha_i>}\right] , \qquad (7)$$

where $<\alpha_i>$ is the average over the range of input attenuation values in dB and, in the present work, for a range of 0-12dB, has a value of 6.0. The formula was derived from a mathematical representation of the input/output attenuation procedure described earlier for evaluating deviation from perfect square law behavior.
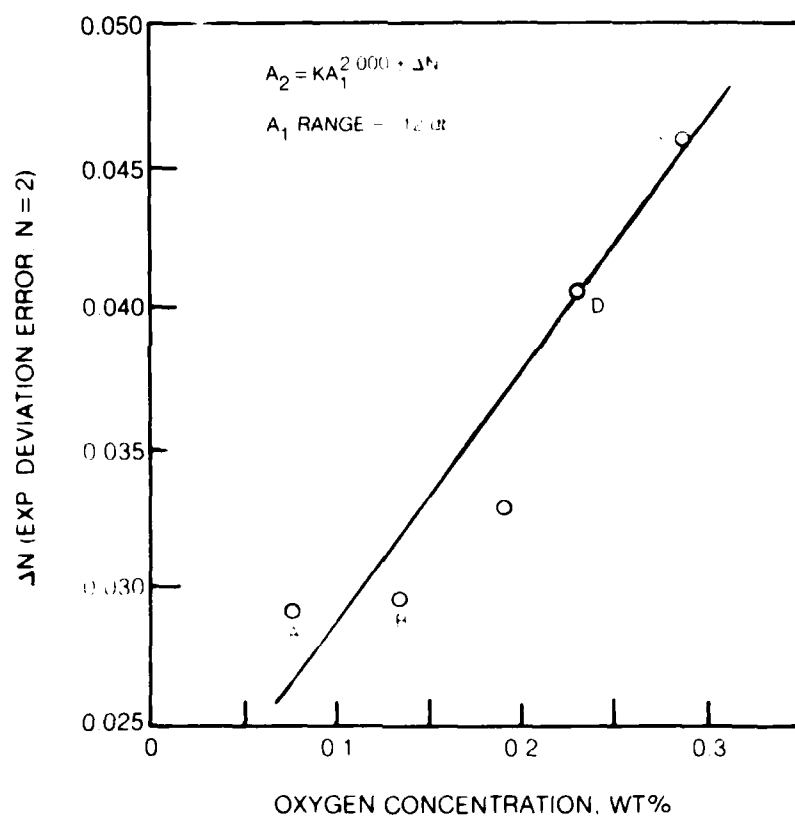
In the earlier work (Ref. 1), a different analysis was used. Although the results are very nearly the same, the present analysis is believed to be more accurate. The result of applying the new analysis procedure to the data of Ref. 1 is shown in Fig. 6.

The present results are shown in Fig. 7. Only a 12 dB range of input amplitude was used in the present study due to the 2% constraint on system linearity. The deviation is similar to that observed in the Ref. 1 study but has approximately twice the slope. The increased slope may be attributed to the increased specimen grain size. The residual deviation at zero oxygen concentration most likely arises from oxygen-independent grain size effects such as those observed by Jon, et al (Ref. 5) since the system non-linearity, remaining constant for each oxygen concentration, does not contribute to the differential change in exponent.

16

FIG. 6

## SQUARE LAW DEVIATION FOR REF. 1 DATA

$A_2 = KA_1^{2.000} \pm \Delta N$

A_1 RANGE — 16 db

(Plot: y-axis "ΔN (EXP. DEVIATION ERROR, N = 2)" ranging 0.009 to 0.021; x-axis "OXYGEN CONCENTRATION, WT %" ranging 0 to 0.3; data points A, B, C, D, E)

FIG. 7

SQUARE LAW DEVIATION FOR CURRENT STUDY DATA

$A_2 = KA_1^{2.000} + \Delta N$

A_1 RANGE —

OXYGEN CONCENTRATION, WT%

83—8—13—5

18

To evaluate the third harmonic data, it was necessary, as discussed previously, to study the attenuations of the fundamental and third harmonics. The results are shown in Fig. 8. Attenuation data were taken at 5, 10 and 15 MHz for three different locations on each of the five specimens. The three attenuations for each specimen at each frequency were averaged. The spread of values on each specimen is shown about the mean attenuation of all five specimens by the hatched region. The results in Fig. 8 show the variation of attenuation on any given specimen is as great as the variation between the five. There is, nevertheless, a weak correlation between increasing attenuation levels over the frequency range and oxygen concentration. Specimen C deviates most strongly from this correlation. Note that specimen C also shows the greatest deviation in the square law data of Fig. 7. The data tends to flatten out at higher frequencies suggesting that scattering from grains is evolving from the frequency-squared dependent phase scattering regime to the frequency-independent diffusion scattering regime. To verify this, the five specimens were chemically etched using a 1-2 solution (97% water, 2% nitric acid, 1% hydroflouric acid). The average grain sizes were microscopically evaluated against standard grain-size charts with the results shown in Fig. 9. The grain sizes are similar in dimension to the wavelength at the higher frequencies, thus verifying diffusion scattering as the dominant attenuation mechanism at these frequencies. Note that specimen C is the only one falling outside the apparent correlation of grain size to oxygen content. Specimen C was observed to have a very wide distribution of grain sizes compared to the relatively narrow distributions in the other specimens. This grain size anomaly correlates with the excessive square law deviation and attenuation shown by specimen C, and suggests that grain size in general plays a role in the square law deviation/oxygen correlation observed. This correlation would tend to strengthen the local residual stress hypothesis since it would imply an excess of oxygen at the grain boundaries. For each specimen, the third harmonic amplitude was measured relative to that of specimen A, the sample having the lowest oxygen concentration. All the data fall within the 15% intrinsic error except for specimen E which shows a 22% deviation.

The attenuation data of Fig. 8 were used to provide corrections for the third harmonic data shown in Fig. 10. The values at 5 and 15 MHz were used with Eqs. 4 and 5 to correct for specimen attenuation from the point of origin of the fundamental. Thus, if there is a weak correlation, it lies within the experimental error for the data reported herein and becomes significant only at, or above, 0.3 weight percent oxygen content.

ATTENUATION AS A FUNCTION OF FREQUENCY FOR Ti SPECIMENS

SPECIMENS
● A
○ B
▽ C
△ D
□ E

83-8-13-7

FIG. 9
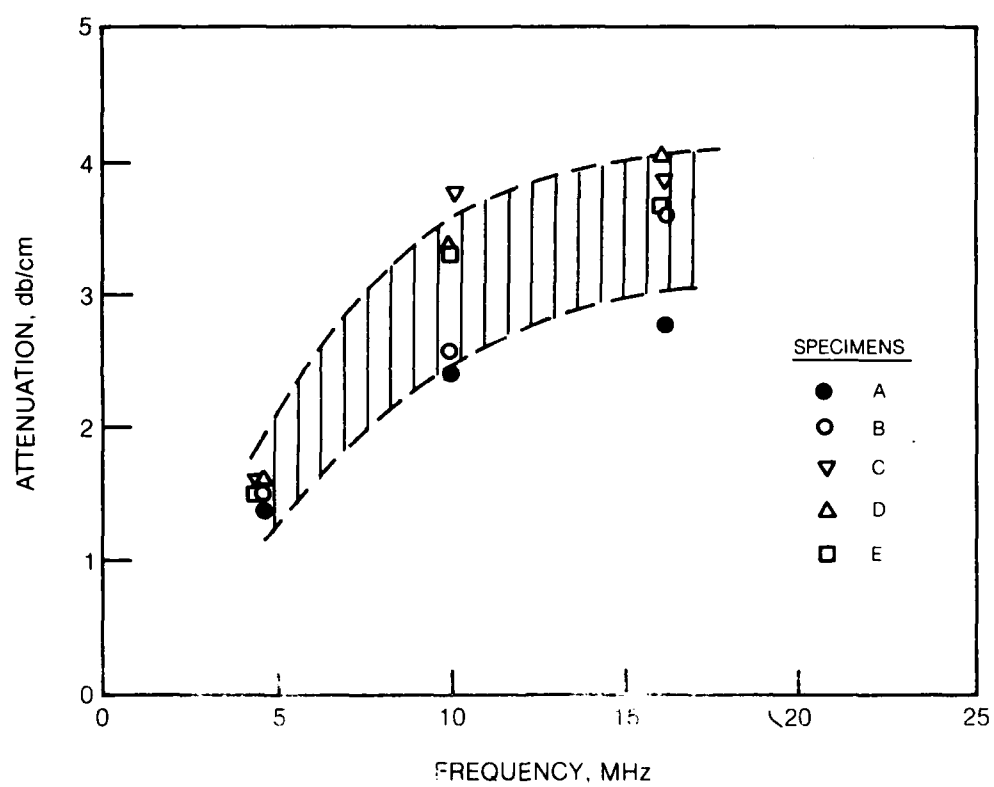
Ti SPECIMEN GRAIN SIZE AS A FUNCTION OF OXYGEN CONTENT

OXYGEN CONCENTRATION, WT %

83—8—13—8

FIG. 10
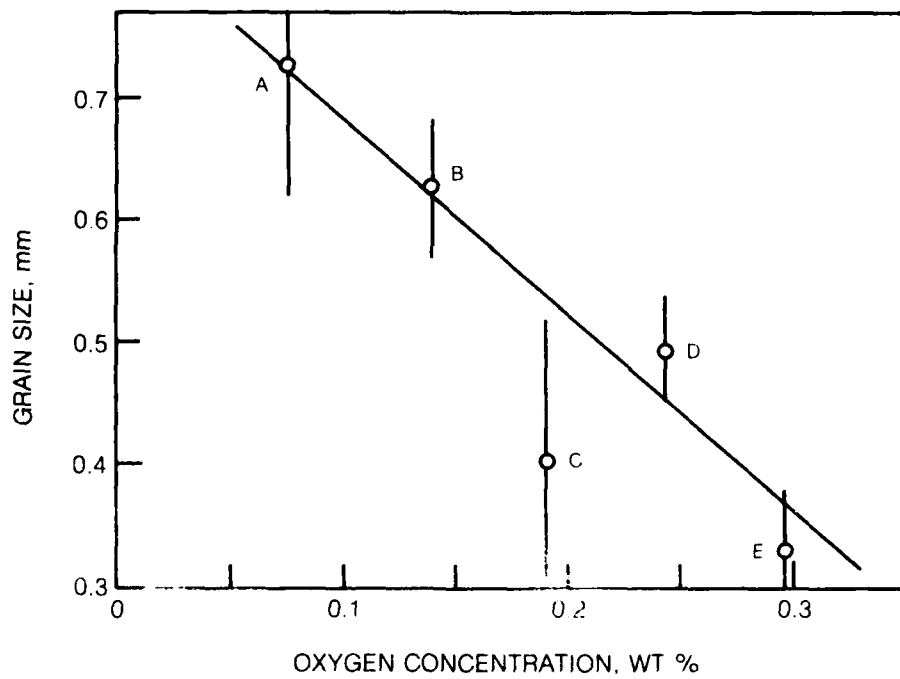
RELATIVE THIRD HARMONIC CONTENT OF ULTRASONIC SIGNAL AS A FUNCTION OF OXYGEN CONTAMINATION

CONSTANT INITIAL AMPLITUDE

83-8-13-9

22
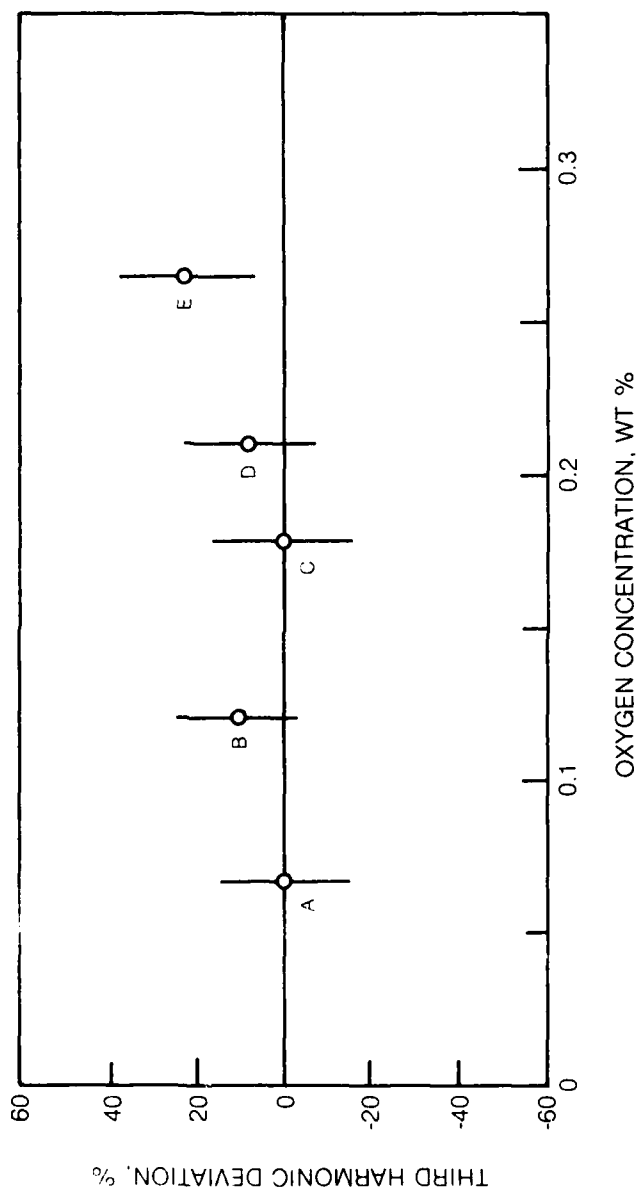
CONCLUDING REMARKS

The correlation of the second harmonic deviation from square law dependence with oxygen content, observed in the Ref.1 study, was confirmed in the present study. It appears, however, that energy transfer to the third harmonic is not responsible for the deviation, since it should have been a much greater effect than that observed in the experiment. A second hypothesis – direct local residual stress influence on the second harmonics – appears to be supported by the grain-size/oxygen data and is consistent with the square law deviation observations. Residual stresses are much more difficult to control and quantify. Further studies are required to verify this hypothesis in relation to grain size and effects on second harmonic generation. The present work also indicates it may be necessary to know both the specimen average grain size and the extent of square law deviation to evaluate the oxygen content.

REFERENCES

1. Ringermacher, H. I. and R. S. Williams: Nonlinear Ultrasonic
    Characterization of Oxygen in Titanium. NRL Final Report, Contract
    N00014-81-C-2426.   UTRC Report R82-995862, March 1982.

2. Sargent, G. A., and H. Conrad: On the Strengthening of Titanium by
    Oxygen. Scripta Metallurgica 6, 1099 (1972).

3. Gupta, D., and S. Weinig: The Dislocation-Oxygen Interaction in Alpha
    Titanium and Its Effects on the Ductile-to-Brittle Transition. Trans.
    of the Metallurigical Soc. of AIME 215, 209 (1959).

4. Hsu, N., and H. Conrad: Ultrasonic Wave Velocity Measurements on
    Titanium-Oxygen Alloys. Scripta Metallurgica 5, 905 (1971).

5. Jon, M. D., W. P. Mason, and D. N. Beshers: Observation of Acoustic
    Harmonics Generated by Long Range Motion of Dislocations. J Appl. Phys.
    49, 5871 (1978).

6. Granato, A., and K. Lucke: Theory of Mechanical Damping Due to
    Dislocations. J. Appl. Phys. 27, 583 (1956).

7. Hikata, A., and C. Elbaum: Generation of Ultrasonic Second and Third
    Harmonics Due to Dislocations. I, Phys. Rev. 144, 469 (1966).

8. Hikata, A., F. A. Sewell, Jr., and C. Elbaum: Generation of Ultrasonic
    Second and Third Harmonics Due to Dislocations. II, Phys. Rev. 151, 422
    (1966).

END

FILMED

9-84

DTIC